



Published in final edited form as:

*J Am Chem Soc.* 2017 August 23; 139(33): 11427–11433. doi:10.1021/jacs.7b03540.

## ***In Vivo* Structure-Activity Relationships and Optimization of an Unnatural Base Pair for Replication in a Semi-Synthetic Organism**

**Aaron W. Feldman and Floyd E. Romesberg\***

Department of Chemistry, The Scripps Research Institute, 10550 North Torrey Pines Road, La Jolla, California 92037, USA

### **Abstract**

In an effort to expand the genetic alphabet and create semi-synthetic organisms (SSOs) that store and retrieve increased information, we have developed the unnatural base pairs (UBPs) **dNaM** and **d5SICS** or **dTPT3** (**dNaM-d5SICS** and **dNaM-dTPT3**). The UBPs form based on hydrophobic and packing forces, as opposed to complementary hydrogen bonding, and while they are both retained within the *in vivo* environment of an *E. coli* SSO, their development was based on structure-activity relationship (SAR) data generated *in vitro*. To address the likely possibility of different requirements of the *in vivo* environment, we screened 135 candidate UBPs for optimal performance in the SSO. Interestingly, we find that *in vivo* SARs differ from those collected *in vitro*, and most importantly, we identify four UBPs whose retention in the DNA of the SSO is higher than that of **dNaM-dTPT3**, which was previously the most promising UBP identified. The identification of these four UBPs further demonstrates that when optimized, hydrophobic and packing forces may be used to replace the complementary hydrogen bonding used by natural pairs and represents a significant advance in our continuing efforts to develop SSOs that store and retrieve more information than natural organisms.

### **Graphical abstract**

---

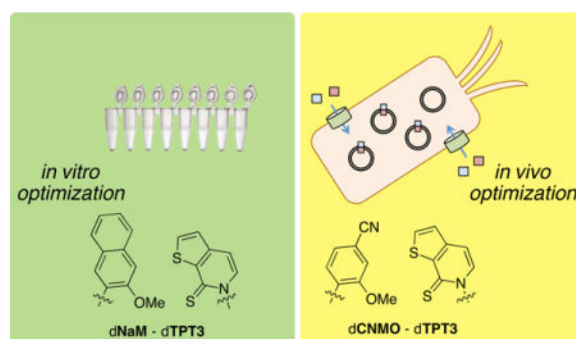
\*Corresponding Author: floyd@scripps.edu.

#### **Supporting Information**

The Supporting Information is available free of charge on the ACS Publications website. Additional methods, supporting tables and figures, and references (PDF)

#### **Author Contributions**

All authors have given approval to the final version of the manuscript.



## INTRODUCTION

Natural organisms store genetic information in an alphabet of four nucleotide “letters,” and the replication and retrieval of this information is mediated by their selective pairing to form two base pairs. The addition of two new letters that form an unnatural base pair (UBP) would increase the potential information content and lay the foundation for semi-synthetic organisms (SSOs) capable of producing proteins with unnatural amino acids or even possessing novel forms and functions, which is the central goal of synthetic biology.<sup>1</sup> We,<sup>2</sup> as well as the Benner<sup>3</sup> and Hirao<sup>4</sup> groups, have worked towards this goal and have each identified UBPs that are well replicated *in vitro*. Our efforts have focused upon a family of UBPs represented by dNaM-d5SICS and dNaM-dTPT3 (Figure 1), which utilize hydrophobic and packing forces, as opposed to complementary hydrogen bonding, to stably pair within duplex DNA and during replication.<sup>5–10</sup> This mode of pairing results in an edge-to-edge, Watson-Crick-like geometry during unnatural triphosphate insertion within the polymerase active site, but cross-strand intercalation once the UBP is synthesized,<sup>11–13</sup> which likely mandates deintercalation for continued synthesis. Thus, the extended aromatic surface area of the unnatural nucleobases may be a liability. Nonetheless, with the unnatural triphosphates imported via transgenic expression of the nucleoside triphosphate transporter *PNTT2*, we developed an *Escherichia coli* SSO that stably retains these UBPs in its DNA.<sup>10,14</sup> While the retention of the UBPs in the DNA of the SSO is not equivalent to that of a natural base pair, retention may be raised to natural-like levels through the action of Cas9 targeted to degrade the DNA that has lost the UBP.<sup>14</sup>

Both the dNaM-d5SICS and dNaM-dTPT3 UBPs were identified from an intensive investigation of over 150 analogs that were evaluated *in vitro*, initially via steady-state kinetics and later by retention in PCR-amplified DNA.<sup>2</sup> These studies provided the key structure-activity relationship (SAR) data used to optimize the unnatural nucleotides, but the *in vivo* environment of the SSO introduces additional constraints, such as toxicity, import, and polymerase availability. Thus, it is unclear whether UBPs optimized based on *in vitro* SAR are optimal for performance *in vivo*. Indeed, during *in vitro* optimization, we emphasized the importance of identifying multiple different UBPs whose constituent nucleotides possess varying physicochemical properties to provide flexibility during the effort to deploy them in an SSO.<sup>8,15</sup>

To extend our SAR data to include the restraints of the *in vivo* SSO environment, we conducted a screen for pairs of unnatural triphosphates that when added to growth media support high level UBP retention. From an examination of 135 candidate UBPs, we generate new SAR data that differs in several interesting ways from that generated *in vitro*, and remarkably, at least in some cases demonstrates that replication is more permissive *in vivo* than *in vitro*. Most importantly, we discover four new UBPs that are more efficiently retained *in vivo* than either dNaM-d5SICS or dNaM-dTPT3. One of the constituent nucleobases in each of the new UBPs is dTPT3, suggesting that it represents an at least currently optimal solution, but it is paired with different dNaM analogs. The most promising new UBP is retained in sequences where neither dNaM-d5SICS nor dNaM-dTPT3 is retained even with Cas9, and thus represents the most promising UBP identified to date for use in our continuing efforts to develop an SSO that stably stores increased information.

## EXPERIMENTAL SECTION

### General

All bacteria were cultured in 100  $\mu$ L of liquid 2 $\times$ YT media (casein peptone 16 g/L, yeast extract 10 g/L, NaCl 5 g/L) supplemented with potassium phosphate (50 mM, pH 7) in 96-well microwell plates. When noted, antibiotics were used at the following concentrations: chloramphenicol, 5  $\mu$ g/mL; ampicillin, 100  $\mu$ g/mL. Cell growth, indicated as OD<sub>600</sub>, was measured using a Perkin Elmer EnVision 2103 Multilabel Reader with a 590/20 nm filter. Unless otherwise stated, molecular biology reagents were purchased from New England Biolabs (Ipswich, MA) and were used according to the manufacturer's protocols. As necessary, purification of nucleic acids was accomplished by microelution columns (Zymo Research Corp; Irvine, CA). All natural oligonucleotides were purchased from IDT (San Diego, CA), and oligonucleotides containing dNaM were synthesized by Biosearch Technologies (Petaluma, CA) with purification by reverse phase cartridge and were kindly provided by Synthorx (La Jolla, CA). Unnatural nucleotide triphosphates were prepared as previously described (Table S2), and confirmed by MALDI-TOF and UV/Vis.

### Analysis of UBP Retention

Plasmids containing the dNaM-dTPT3 UBP were prepared and used to transform *E. coli* strain YZ3 as described previously.<sup>10,14</sup> Following transformation, the SSO was allowed to recover at 37 °C for 1 h in media containing dNaMTP (125  $\mu$ M) and dTPT3TP (25  $\mu$ M). Cells were pelleted by centrifugation, resuspended in fresh media lacking unnatural triphosphates, and then used to inoculate cultures containing different pairs of unnatural triphosphates at the specified concentrations. When the cell density reached an OD<sub>600</sub> of ~0.7, cells were pelleted and plasmids were recovered and PCR amplified with d5SICSTP and a biotinylated analog of dNaMTP, and UBP retention was determined by comparing the intensity of the streptavidin shifted and unshifted bands via PAGE as described previously<sup>10,14</sup> and in Supporting Information. Plasmids with the dNaM-dTPT3 UBP were used as a starting point for the *in vivo* replication experiments to eliminate the need to construct separate plasmids for every candidate UBP examined and to eliminate differences in UBP retention during *in vitro* plasmid construction. We note that this requires each dNaM analog to pair with dTPT3 and each dTPT3 analog to pair with dNaM during the first round

of replication, and similar pairing is required for the first round amplification during PCR analysis. It should also be noted that this assay detects bulk retention, and inversion of the pair by, for example, self-pairing, is not excluded.

## RESULTS

To create a template for *in vivo* replication assays, Golden Gate assembly was used to construct a derivative of the pUC19 plasmid in which a single dNaM-dTPT3 UBP was embedded within the TK1 sequence (local sequence AXT, X = dNaM; referred to hereafter as sequence context **1**), a context within which the dNaM-dTPT3 UBP is well replicated in our SSO.<sup>14</sup> Plasmids were then used to transform the SSO, which was allowed to recover briefly in media containing dNaMTP and dTPT3TP. Upon resuspension in fresh media lacking triphosphates, the SSO culture was split into 100- $\mu$ L aliquots and supplemented with varying concentrations of different pairs of unnatural triphosphates. Once the cultures reached an OD<sub>600</sub> of ~0.7, plasmids were recovered and analyzed for UBP retention (Figure 2).

In a first phase of screening we explored the addition of 25  $\mu$ M of dTPT3TP and one of 75 different dNaMTP analogs (structures shown in Figure 3A) added at a concentration of 125  $\mu$ M or 10  $\mu$ M. After plasmid recovery, we observed UBP retention of >90% with thirteen analogs (dMMO2TP, dDMOTP, dNaMTP, dCIMOTP, dCNMOTP, d5FMTP, dFDMOTP, dFIMOTP, dZMOTP, dIMOTP, dMIMOTP, dFEMOTP, and dMMO2<sup>A</sup>TP) (Figure 4A and Supporting Information). Of the remaining analogs, four showed a retention of 50–90% (d2OMeTP, dTfMOTP, dMEMOTP, dVMOTP), nine showed a retention of 20–50% (dDM5TP, d2MNTP, d45DMPyTP, dEMOTP, dDMTP, dTOK581TP, dTOK587TP, dPyMO2TP, d35DMPyTP), and the remainder showed a retention of less than 20%. Addition of the dNaMTP analogs at the lower concentration resulted in generally less efficient UBP retention, with only four, dMMO2TP, dCIMOTP, dCNMOTP, and d5FMTP, resulting in high retention (>80%). Five, dFIMOTP, dIMOTP, dFEMOTP, dMMO2<sup>A</sup>TP, as well as dNaMTP itself, showed intermediate levels of retention (between 40–80%), and four, dFDMOTP, dVMOTP, d2OMeTP, and dZMOTP, showed slightly less retention (20–40%), with the remainder showing <20% retention.

We next explored UBP retention with the addition of 125  $\mu$ M dNaMTP and one of 16 different dTPT3TP analogs (structures shown in Figure 3B) at a concentration of 125  $\mu$ M or 10  $\mu$ M. When provided at the higher concentration, nine of the dTPT3TP analogs, dTPT3<sup>PA</sup>TP, dTPT3TP, dSICSTP, dFPT1, d4SICS, dTPT1, d5SICS, dNICS, and dSNICS, showed significant UBP retention upon plasmid recovery (Figure 4B and Supporting Information). Unlike with the dNaMTP analogs, these nine UBPs showed similar or better retention when provided at the lower concentration, while dICSTP, d4MICSTP, and d5MICSTP also showed significant retention (retention of these three analogs could not be determined at higher concentrations due to toxicity). Clearly UBP retention is more optimal with the lower concentration of these analogs, and under these conditions, when combined with dNaMTP, all triphosphate analogs examined except dONICSTP, d7OTPTP, d7OFPTP, and d4OTPTP (which were toxic at both concentrations) showed retention of the UBP in excess of 70%.

In a second phase of screening, we crossed the twelve most promising dTPT3TP analogs with the four most promising dNaMTP analogs identified in the first phase. We incorporated the UBP within the same plasmid, but embedded it within a local sequence of AXA (context 2, X = dNaM), a context in which we have found retention of dNaM-dTPT3 to be more challenging than sequence context 1.<sup>14</sup> Based on the first phase of screening, we also focused on concentrations of the dNaMTP and dTPT3TP analogs of 25  $\mu$ M and 10  $\mu$ M, respectively, to increase the dynamic range of the screen. Significant retention was only observed with pairs containing dTPT3TP or dSICSTP, but each was found to yield at least moderate retention with each of the four dNaMTP analogs (Figure 4C and Supporting Information). Retention with dSICSTP was moderate when paired with dMMO2TP (19%), but more significant with d5FMTP, dCNMOTP, and dCIMOTP, with 68%, 79%, and 61% retention, respectively. The highest retentions, however, were observed with dTPT3TP (all >87%).

Next we explored retention with the four most promising UBPs identified, d5FM-dTPT3, dMMO2-dTPT3, dCNMO-dTPT3, and dCIMO-dTPT3, when embedded within context 2, but with unnatural triphosphate concentrations of 25  $\mu$ M, 10  $\mu$ M, or 2.5  $\mu$ M (Figure 5). While it was clear that dMMO2TP and d5FMTP were retained best at 25  $\mu$ M, UBP retention was too high to differentiate in the case of dCNMOTP and dCIMOTP. Thus, we examined retention with the UBP positioned in the same plasmid, but within the local sequence context of CXC (context 3, X = dNaM), which is particularly challenging for dNaM-dTPT3 retention<sup>14</sup> (Figure 5). The data reveal that 25  $\mu$ M is the most optimal concentration for both pairs and that dCNMOTP and dTPT3TP perform better than dCIMOTP and dTPT3TP, with retentions of 42% and 21%, respectively. While d5FMTP and dMMO2TP resulted in slightly higher retention in this sequence context at high concentration (49% and 45%, respectively), they resulted in significantly less retention at the lower concentrations.

Of the 135 candidate UBPs examined, the data reveal that dCNMO-dTPT3 is most efficiently replicated in the SSO. To directly and more thoroughly compare this UBP with dNaM-dTPT3, the most efficiently replicated UBP previously identified, we examined retention of both pairs in the three sequence contexts described above, as well as a fourth, which positions the UBP within the local sequence context of CXG (context 4), which is one of the most challenging sequences for dNaM-dTPT3<sup>14</sup> (Figure 6). dTPT3TP was added at a fixed concentration of 25  $\mu$ M, while dNaMTP or dCNMOTP was added at a concentration of either 125  $\mu$ M or 25  $\mu$ M. At the higher concentration, we observed >99% retention in sequence context 1 with both dCNMOTP and dNaMTP, but while retention remained high with dCNMOTP added at the lower concentration (98%), it was decreased with dNaMTP (85%). In context 2, reduced retention was observed with dNaMTP at both the high concentration (73%) and the low concentration (36%), but retention at both concentrations remained high with dCNMOTP (>99%). In context 3, addition of dNaMTP at the higher concentration resulted in only moderate retention (26%), while addition at the lower concentration resulted in no retention. However, with dCNMOTP, significant retention was observed at both high (65%) and low concentrations (42%). Finally, with context 4, the UBP

was not retained significantly at either concentration with dNaMTP, but remained moderate at high concentrations of dCNMOTP (24%).

## DISCUSSION

The discovery of dNaM-dTPT3 was driven by *in vitro* SARs that ultimately drew on over 150 unnatural nucleotides. While dNaM-dTPT3 was the most promising UBP discovered, and is clearly suitable for use within a living SSO,<sup>14</sup> its retention is sequence context-dependent, with some sequences showing high retention and others less or none. During the *in vitro* discovery phase we also identified variants whose constituent nucleotides have distinct physicochemical properties that may differentiate performance *in vivo*. With these analogs, we have now examined 135 variant UBPs within the *in vivo* environment of our SSO. Interestingly, we find *in vivo* SARs that are both similar to and different from those collected *in vitro*. For example, dICS, and its methyl-derivatized analogs d4MICS and d5MICS, support UBP retention *in vivo* reasonably well, but only at low concentration, suggesting that they are misincorporated opposite natural nucleotides at high concentrations, thereby resulting in stalled replication forks and toxicity. Indeed, *in vitro*, steady state kinetic analyses suggest that these analogs can be misinserted opposite natural nucleotides in a template with reasonable efficiency.<sup>16</sup> However, UBPs containing these analogs cannot be PCR amplified, suggesting that the observed retention is unique to the *in vivo* environment. Heteroatom derivatization of the dICS scaffold is generally deleterious and results in significant toxicity, again consistent with misincorporation, as we observed previously *in vitro*.<sup>17</sup> An exception is dNICS, as this heteroatom-derivatized analog of dICS supports UBP retention reasonably well, and in fact, the additional sulfur substituent of dSNICS results in an analog that supports moderate retention at both low and high concentrations. The beneficial effect of the sulfur does not depend on aza substitution as retention is also increased with dSICS compared to dICS. Thus, the aza and sulfur substituents appear to independently reduce mispairing *in vivo*. While this was observed *in vitro* for the sulfur substituent, the opposite was observed with aza substitution, suggesting that its ability to reduce mispairing is unique to the *in vivo* environment.

The modification of unnatural nucleotides with linkers that allow for site-specific attachment of different functionalities is of particular interest for *in vivo* labeling experiments. Linker modification of dTPT3TP, resulting in dTPT3<sup>PA</sup>TP, is well tolerated *in vivo*, as was also observed *in vitro*. However dMMO2<sup>A</sup>TP is reasonably well tolerated *in vivo*, while dMMO2<sup>PA</sup>TP, dMMO2<sup>BIO</sup>TP and dMMO2<sup>SSBIO</sup>TP completely ablate retention, contrary to what is observed *in vitro*.<sup>18</sup> While dMMO2<sup>A</sup>TP shows a decrease in retention at low concentration, which dTPT3<sup>PA</sup>TP does not, its free amine linker should facilitate *in vivo* labeling or crosslinking experiments. Similarly, dZMOTP and dFEMOTP are well retained *in vivo* when supplemented at high concentrations, and provide an azide and alkyne moiety in the major groove, respectively, where they should also facilitate *in vivo* labeling or crosslinking.

A large body of *in vitro* SAR data demonstrates convincingly that an H-bond acceptor positioned *ortho* to the glycosidic bond, and thus oriented into the developing minor groove upon incorporation into DNA, is generally required for efficient continued primer

elongation.<sup>19</sup> The general requirement of an H-bond acceptor at this position is consistent with studies of natural base pairs,<sup>20–23</sup> which invariably have a similarly disposed H-bond acceptor that is thought to engage in critical interactions with polymerase-based H-bond donors.<sup>24</sup> An exception is the relatively efficient PCR amplification of DNA containing d2MN paired opposite dTPT3.<sup>8</sup> *In vivo*, d2MNTP also supports retention with dTPT3TP, but when combined with dTPT3TP, dDM5TP does as well. Moreover, while dICSTP, dNICSTP, d4MICSTP, and d5MICSTP do not support PCR amplification when paired with any analog,<sup>8</sup> they support reasonable retention *in vivo* when paired dNaMTP. Clearly, the requirements for the *ortho* group are somewhat different *in vitro* and *in vivo*, and at least in some cases, they are more permissive *in vivo*.

From a practical perspective, the most important results of the current study are the excellent *in vivo* performance of the d5FM-dTPT3, dMMO2-dTPT3, dCNMO-dTPT3, and dCIMO-dTPT3 UBPs (Figure 7). Retention of each of these new UBPs in the SSO, in particular, dCNMO-dTPT3, is better than that of dNaM-dTPT3, the previously most promising UBP identified, and requires the addition of less nucleotide triphosphate to the growth media. In fact, dCNMO-dTPT3 shows at least moderate retention in sequence context **4**, where dNaM-dTPT3 is retained so poorly that it cannot be rescued by Cas9, suggesting that it is lost immediately upon attempted replication. Interestingly, this contrasts with *in vitro* data where retention of dNaM-dTPT3 is better than retention of dCNMO-dTPT3,<sup>8,15</sup> suggesting that *E. coli* provide a unique environment for which dCNMO-dTPT3 is more optimal. Possible contributing factors include *PtNTT2*-mediated uptake, stability within the cell, or recognition by different polymerases that can access the replication fork and actually mediate replication *in vivo*.

Regardless of the specific properties that underlie their performance, it is clear that the present work has identified four new UBPs that now represent the most promising candidates for use in an SSO. These new UBPs further demonstrate the ability of hydrophobic and packing interactions to replace complementary H-bonding as the force underlying information storage. It is interesting that each of the new dNaM analogs bear smaller, single ring nucleobases. While this may have contributed to their *in vivo* performance by facilitating uptake, they are likely to be less prone to cross-strand intercalation, and more likely to adopt edge-to-edge structures. This may also contribute to their more optimal retention, and possibly even facilitate the replication of DNA with higher density UBPs. Only UBP loss was characterized in this study, as mutations involving natural nucleotides are predicted to be most problematic.<sup>5,25,26</sup> However, cross-strand intercalation may also facilitate self-pairing, which even at low levels could cause UBP inversion (where the individual nucleotides switch strands). Whatever its level, self-pairing mediated UBP inversion may be less likely with these analogs. Finally, the performance of each of the new UBPs is likely to be even further improved by use of Cas9, and we are currently exploring this possibility. The availability of a family of UBPs that are well retained in the *in vivo* environment of the SSO, but that also possess distinct physicochemical properties, is of great significance as our efforts to retrieve the increased information via transcription and translation will likely introduce additional requirements and restraints.

## Supplementary Material

Refer to Web version on PubMed Central for supplementary material.

## Acknowledgments

This work was supported by the National Institutes of Health (Grant Nos. GM060005 and GM118178 to F.E.R.). A.W.F. was supported by a National Science Foundation Graduate Research Fellowship (Grant No. NSF/DGE-1346837).

## References

1. Leduc, S. *The Mechanisms of Life*. Rebman Company; New York: 1911.
2. Malyshev DA, Romesberg FE. *Angew Chem Int Ed*. 2015; 54:11930–11944.
3. Zhang L, et al. *J Am Chem Soc*. 2015; 137:6734–6737. [PubMed: 25966323]
4. Kimoto, M., Hirao, I. *Chemical Biology of Nucleic Acids: Fundamentals and Clinical Applications*. Erdmann, AV, Markiewicz, TW., Barciszewski, J., editors. Springer Berlin Heidelberg; Berlin, Heidelberg: 2014. p. 131–148.
5. Leconte AM, Hwang GT, Matsuda S, Capek P, Hari Y, Romesberg FE. *J Am Chem Soc*. 2008; 130:2336–2343. [PubMed: 18217762]
6. Lavergne T, Malyshev DA, Romesberg FE. *Chem Eur J*. 2012; 18:1231–1239. [PubMed: 22190386]
7. Malyshev DA, Dhami K, Quach HT, Lavergne T, Ordoukhanian P, Torkamani A, Romesberg FE. *Proc Natl Acad Sci USA*. 2012; 109:12005–12010. [PubMed: 22773812]
8. Dhami K, Malyshev DA, Ordoukhanian P, Kubelka T, Hocek M, Romesberg FE. *Nucleic Acids Res*. 2014; 42:10235–10244. [PubMed: 25122747]
9. Li L, Degardin M, Lavergne T, Malyshev DA, Dhami K, Ordoukhanian P, Romesberg FE. *J Am Chem Soc*. 2014; 136:826–829. [PubMed: 24152106]
10. Malyshev DA, Dhami K, Lavergne T, Chen T, Dai N, Foster JM, Correa IR Jr, Romesberg FE. *Nature*. 2014; 509:385–388. [PubMed: 24805238]
11. Betz K, Malyshev DA, Lavergne T, Welte W, Diederichs K, Dwyer TJ, Ordoukhanian P, Romesberg FE, Marx A. *Nat Chem Biol*. 2012; 8:612–614. [PubMed: 22660438]
12. Betz K, Malyshev DA, Lavergne T, Welte W, Diederichs K, Romesberg FE, Marx A. *J Am Chem Soc*. 2013; 135:18637–18643. [PubMed: 24283923]
13. Malyshev DA, Pfaff DA, Ippoliti SI, Hwang GT, Dwyer TJ, Romesberg FE. *Chem Eur J*. 2010; 16:12650–12659. [PubMed: 20859962]
14. Zhang Y, Lamb BM, Feldman AW, Zhou AX, Lavergne T, Li L, Romesberg FE. *Proc Natl Acad Sci U S A*. 2017; 114:1317–1322. [PubMed: 28115716]
15. Lavergne T, Degardin M, Malyshev DA, Quach HT, Dhami K, Ordoukhanian P, Romesberg FE. *J Am Chem Soc*. 2013; 135:5408–5419. [PubMed: 23547847]
16. Wu Y, Ogawa AK, Berger M, McMinn DL, Schultz PG, Romesberg FE. *J Am Chem Soc*. 2000; 122:7621–7632.
17. Henry AA, Yu C, Romesberg FE. *J Am Chem Soc*. 2003; 125:9638–9646. [PubMed: 12904030]
18. Seo YJ, Malyshev DA, Lavergne T, Ordoukhanian P, Romesberg FE. *J Am Chem Soc*. 2011; 133:19878–19888. [PubMed: 21981600]
19. Matsuda S, Leconte AM, Romesberg FE. *J Am Chem Soc*. 2007; 129:5551–5557. [PubMed: 17411040]
20. Spratt TE. *Biochemistry*. 2001; 40:2647–2652. [PubMed: 11258875]
21. Meyer AS, Blandino M, Spratt TE. *J Biol Chem*. 2004; 279:33043–33046. [PubMed: 15210707]
22. Morales JC, Kool ET. *J Am Chem Soc*. 1999; 121:2323–2324. [PubMed: 20852718]
23. Morales JC, Kool ET. *Biochemistry*. 2000; 39:12979–12988. [PubMed: 11041863]
24. Li Y, Waksman G. *Protein Sci*. 2001; 10:1225–1233. [PubMed: 11369861]



25. Seo YJ, Hwang GT, Ordoukhanian P, Romesberg FE. *J Am Chem Soc.* 2009; 131:3246–3252. [PubMed: 19256568]
26. Morris SE, Feldman AW, Romesberg FE. *ACS Synth Biol.* 2017; Published online 27 June. doi: 10.1021/acssynbio.7b00115

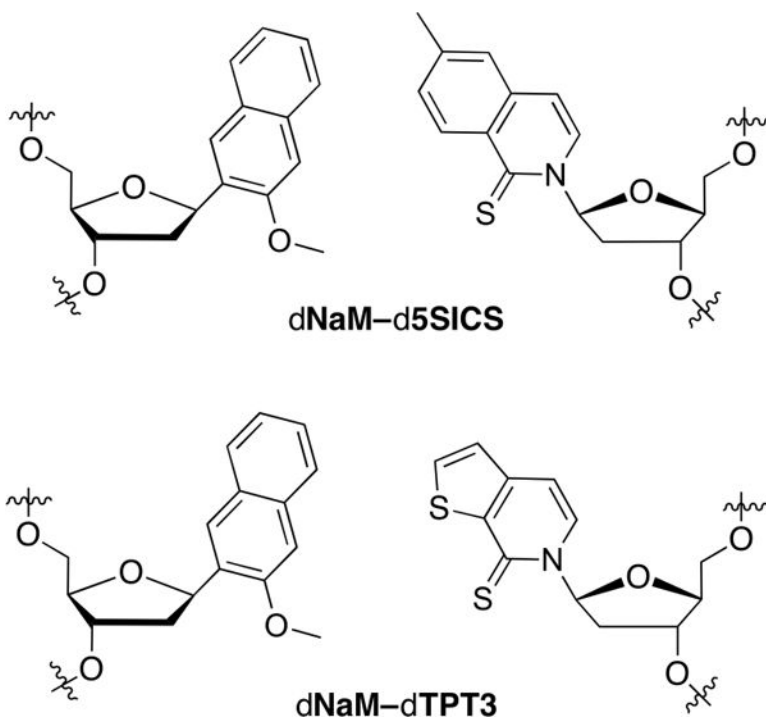


**Figure 1.**  
The dNaM-d5SICS and dNaM-dTPT3 UBPs.

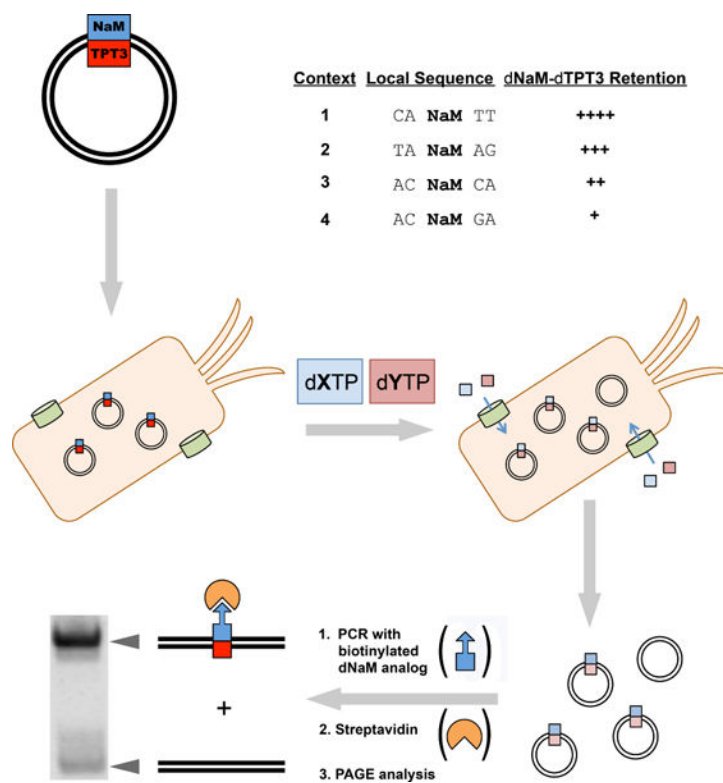


**Figure 2.** Graphical representation of screen workflow. For sequence contexts **1 – 4**, **X** denotes **NaM** or a **NaM** analog and **Y** denotes **TPT3** or a **TPT3** analog. Retention levels of dNaM-dTPT3 are indicated with “+” symbols. See Ref <sup>14</sup> for original report of dNaM-dTPT3 retention data.

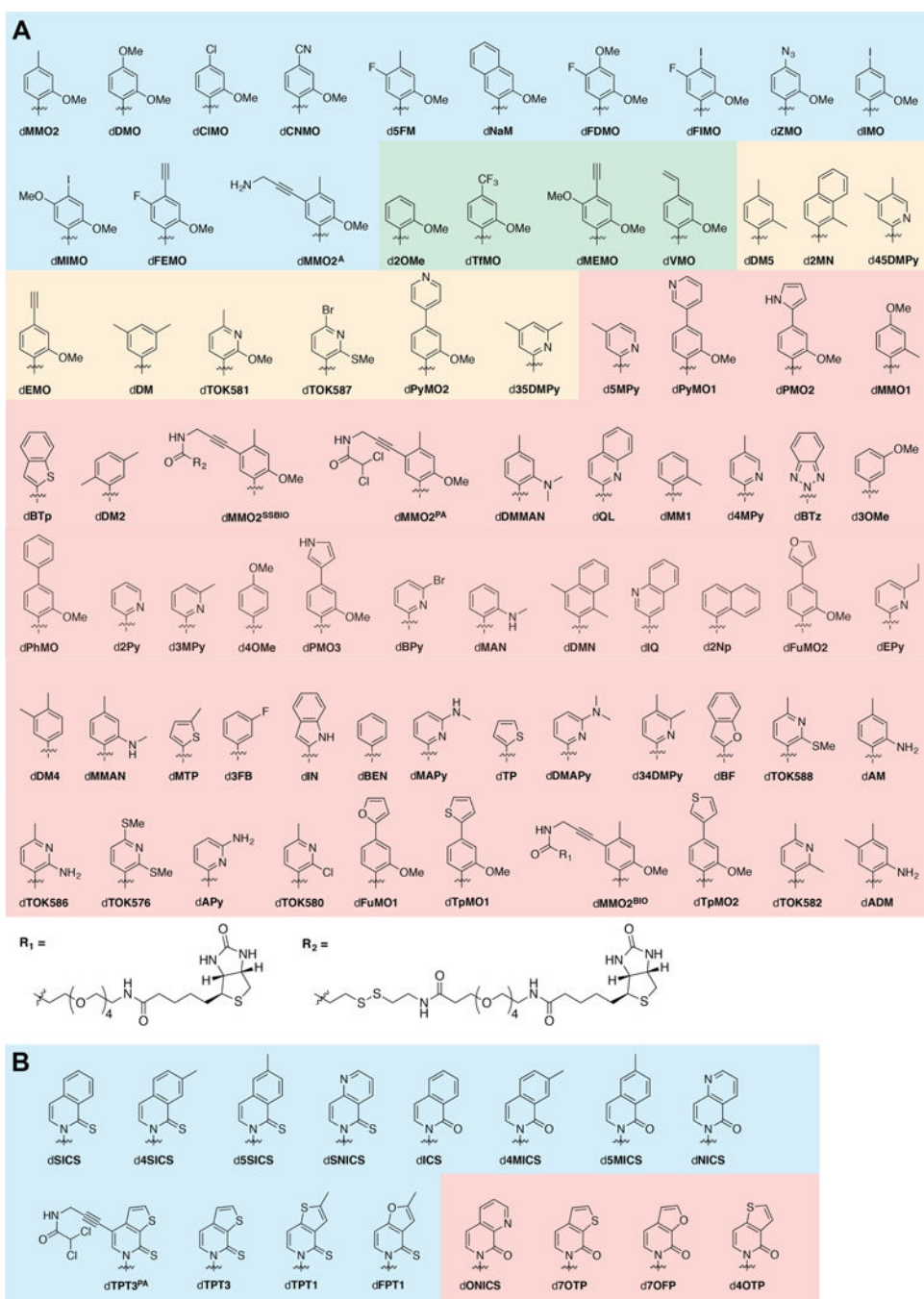


**Figure 3.** Structure of analogs used in current study. **(A)** dNaMTP analogs. Blue shading corresponds to analogs that at 125  $\mu$ M showed greater than 90% retention in phase 1 of the screen. Green shading corresponds to those that at 125  $\mu$ M showed retentions between 50% and 90% in phase 1. Orange shading corresponds to those that at 125  $\mu$ M showed between 20% and 50% retention. Red shading corresponds to those that at 125  $\mu$ M showed less than 20% retention. **(B)** dTPT3 analogs. Blue shading corresponds to those that at 10  $\mu$ M showed greater than 90% retention in phase 1 of the screen and red shading corresponds to those that showed less

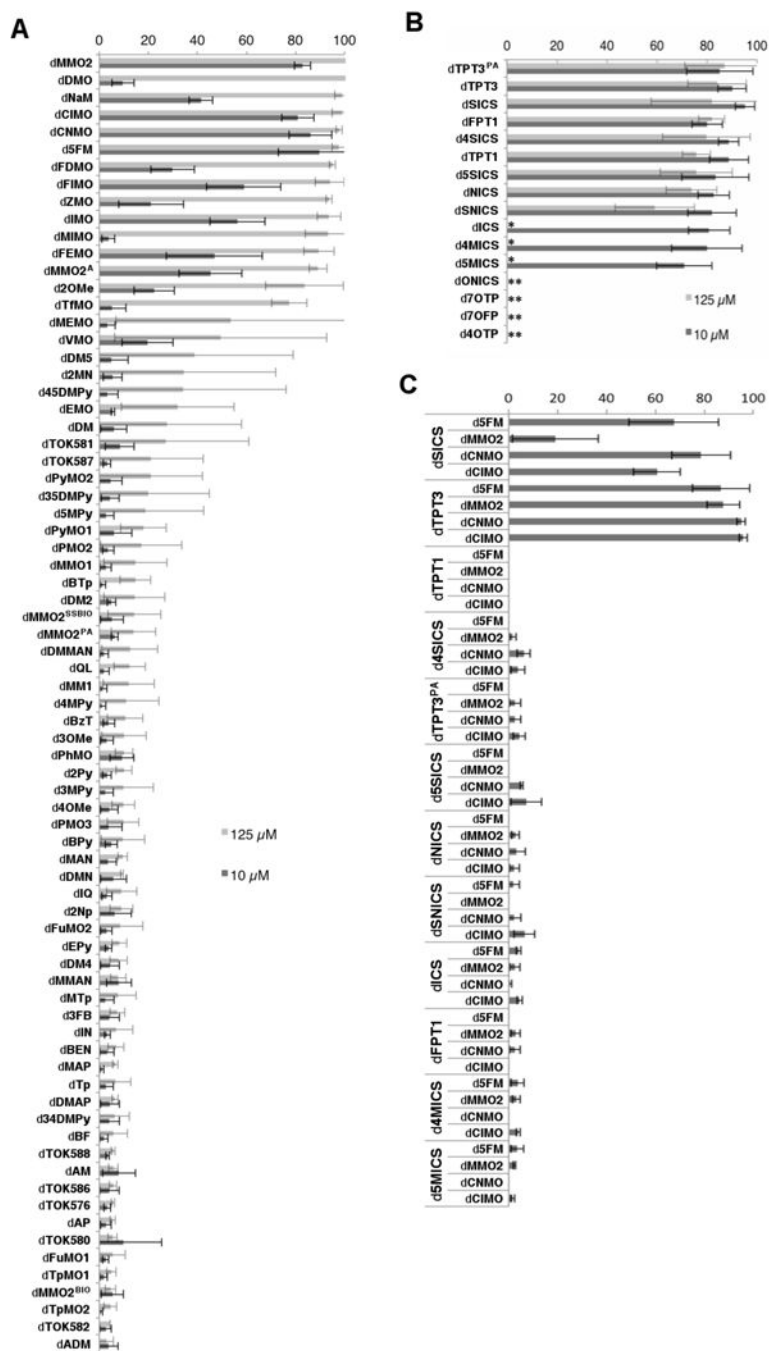
than 10% retention at the same concentration. Ribose and phosphates omitted for clarity. For original references see Supporting Information.

Author Manuscript


Author Manuscript

Author Manuscript

Author Manuscript

**Figure 4.**

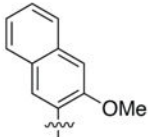
UBP retention (%). (A) dNaMTP analogs added at either 125  $\mu$ M or 10  $\mu$ M and dTPT3TP added at 25  $\mu$ M. (B) dTPT3TP analogs added at either 125  $\mu$ M or 10  $\mu$ M and dNaMTP added at 125  $\mu$ M. (C) Selected analogs screened against each other with dNaMTP analogs added at 25  $\mu$ M and dTPT3TP analogs added at 10  $\mu$ M. Data is an average of 3 independent trials, with error bars indicating standard deviation. A single asterisk indicates that no cell growth was observed at the higher concentration, and a double asterisk indicates that no cell growth was observed at either concentration.



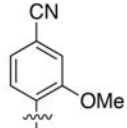
context 2		d5FMTP			dMMO2TP			dCNMOTP			dCIMOTP		
		25 $\mu$ M	10 $\mu$ M	2.5 $\mu$ M	25 $\mu$ M	10 $\mu$ M	2.5 $\mu$ M	25 $\mu$ M	10 $\mu$ M	2.5 $\mu$ M	25 $\mu$ M	10 $\mu$ M	2.5 $\mu$ M
dTPT3TP	25 $\mu$ M	90 $\pm$ 7	95 $\pm$ 3	76 $\pm$ 9	90 $\pm$ 4	86 $\pm$ 11	63 $\pm$ 31	101 $\pm$ 10	103 $\pm$ 1	103 $\pm$ 7	98 $\pm$ 4	92 $\pm$ 4	80 $\pm$ 20
	10 $\mu$ M	87 $\pm$ 12	83 $\pm$ 5	69 $\pm$ 6	88 $\pm$ 7	67 $\pm$ 16	68 $\pm$ 16	101 $\pm$ 8	91 $\pm$ 3	88 $\pm$ 9	92 $\pm$ 7	89 $\pm$ 5	83 $\pm$ 9
	2.5 $\mu$ M	75 $\pm$ 6	61 $\pm$ 27	47 $\pm$ 14	47 $\pm$ 20	54 $\pm$ 19	17 $\pm$ 8	91 $\pm$ 10	82 $\pm$ 24	92 $\pm$ 4	86 $\pm$ 6	84 $\pm$ 7	73 $\pm$ 10
context 3		d5FMTP			dMMO2TP			dCNMOTP			dCIMOTP		
		25 $\mu$ M	10 $\mu$ M	2.5 $\mu$ M	25 $\mu$ M	10 $\mu$ M	2.5 $\mu$ M	25 $\mu$ M	10 $\mu$ M	2.5 $\mu$ M	25 $\mu$ M	10 $\mu$ M	2.5 $\mu$ M
dTPT3TP	25 $\mu$ M	49 $\pm$ 27	33 $\pm$ 16	14 $\pm$ 3	45 $\pm$ 20	36 $\pm$ 12	19 $\pm$ 8	42 $\pm$ 18	25 $\pm$ 22	22 $\pm$ 7	21 $\pm$ 14	20 $\pm$ 7	8 $\pm$ 4
	10 $\mu$ M	27 $\pm$ 14	14 $\pm$ 5	6 $\pm$ 4	22 $\pm$ 10	16 $\pm$ 10	9 $\pm$ 3	35 $\pm$ 8	28 $\pm$ 7	13 $\pm$ 5	14 $\pm$ 5	15 $\pm$ 2	9 $\pm$ 1
	2.5 $\mu$ M	11 $\pm$ 8	10 $\pm$ 5	9 $\pm$ 6	13 $\pm$ 4	10 $\pm$ 3	5 $\pm$ 3	31 $\pm$ 14	22 $\pm$ 10	9 $\pm$ 1	12 $\pm$ 2	7 $\pm$ 4	9 $\pm$ 2

**Figure 5.**

UBP retention (%) with dTPT3TP and different dNaMTP analogs added at varying concentrations to the media. Shading indicates level of UBP retention. Values are the average and standard deviation of three independent determinations.



COc1ccc2ccccc2c1



COc1cccc(C#N)c1

<i>sequence</i>	<b>dNaM</b>		<b>dCNMO</b>	
	125 $\mu$ M	25 $\mu$ M	125 $\mu$ M	25 $\mu$ M
<b>context 1</b>	99 $\pm$ 3	85 $\pm$ 10	99 $\pm$ 8	98 $\pm$ 7
<b>context 2</b>	73 $\pm$ 21	36 $\pm$ 29	100 $\pm$ 10	101 $\pm$ 10
<b>context 3</b>	26 $\pm$ 16	7 $\pm$ 2	65 $\pm$ 7	42 $\pm$ 18
<b>context 4</b>	13 $\pm$ 2	9 $\pm$ 1	24 $\pm$ 13	14 $\pm$ 5

**Figure 6.** UBP retention (%) with 25  $\mu$ M **dTPT3TP** and varying concentrations of **dNaMTP** or **dCNMOTP** added to the media. Shading indicates level of UBP retention. Values are the average and standard deviation of three independent determinations.



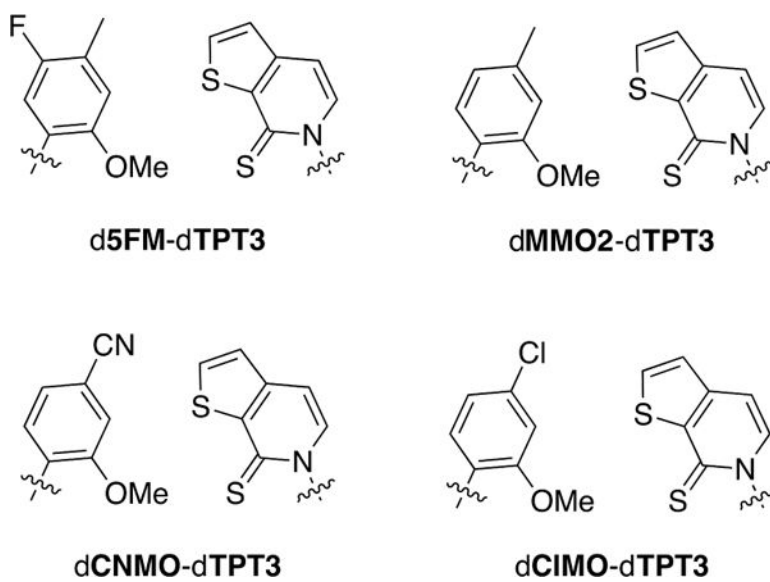


**Figure 7.**  
The four new optimal UBPs discovered.